Remote Sensing of Environment 233 (2019) 111343

Contents lists available at ScienceDirect

Remote Sensing of Environment

journal homepage: www.elsevier.com/locate/rse

Twenty years of satellite and *in situ* observations of surface chlorophyll-*a* from the northern Bay of Biscay to the eastern English Channel. Is the water quality improving?

Francis Gohin[a,*], Dimitry Van der Zande[b], Gavin Tilstone[c], Marieke A. Eleveld[d], Alain Lefebvre[e], Françoise Andrieux-Loyer[a], Anouk N. Blauw[d], Philippe Bryère[e], David Devreker[f], Philippe Garnesson[g], Tania Hernández Fariñas[h], Yoann Lamaury[i], Luis Lampert[a], Héloïse Lavigne[b], Florence Menet-Nedelec[h], Silvia Pardo[c], Bertrand Saulquin[g]

[a] *IFREMER, Laboratoire d'écologie pélagique, DYNECO PELAGOS, CS 10070-29280 Plouzané, France*
[b] *RBINS, 29 rue Vautier, B-1200, Brussels, Belgium*
[c] *PML, Plymouth Marine Laboratory, Prospect Place, West Hoe, Plymouth PL1 3DH, UK*
[d] *Deltares, Marine and Coastal Information Science, P.O. Box 177, 2600, MH, Delft, the Netherlands*
[e] *ARGANS, Bâtiment Le Grand Large, Quai de la douane – 2ème éperon, 29200 Brest, France*
[f] *IFREMER, Laboratoire Environnement et Ressources de Boulogne sur Mer, 150, Quai Gambetta, 62200 Boulogne-sur-Mer, France*
[g] *ACRI-ST, 260 Route du Pin Montard, BP 234, 06904 Sophia-Antipolis, France*
[h] *IFREMER, Laboratoire Environnement et Ressources de Normandie, Av. du Général de Gaulle, BP, 32-14520 Port en Bessin, France*
[i] *Sorbonne Université, Campus Pierre et Marie Curie, 4 place Jussieu, 75005 Paris, France*

ARTICLE INFO

Edited by: Menghua Wang

Keywords:
Satellite remote-sensing
Ocean colour
Phytoplankton
Chlorophyll-a
English Channel
Bay of Biscay
Eutrophication assessment
European marine strategy framework directive

ABSTRACT

The variability of the phytoplankton biomass derived from daily chlorophyll-*a* (Chl-*a*) satellite images was investigated over the period 1998–2017 in the surface waters of the English Channel and the northern Bay of Biscay. Merged satellite (SeaWiFS-MODIS/Aqua-MERIS-VIIRS) Chl-*a* was calculated using the OC5 Ifremer algorithm which is optimized for moderately-turbid waters. The seasonal cycle in satellite-derived Chl-*a* was compared with *in situ* measurements made at seven coastal stations located in the southern side of the English Channel and in the northern Bay of Biscay. The results firstly showed that the satellite Chl-*a* product, derived from a suite of space-borne marine reflectance data, is in agreement with the coastal observations. For compliance with the directives of the European Union on water quality, time-series of 6-year moving average of Chl-*a* were assessed over the region. A clear decline was observed in the mean and 90th percentile of Chl-*a* at stations located in the mixed waters of the English Channel. The time-series at the stations located in the Bay of Biscay showed yearly fluctuations which correlated well with river discharge, but no overall Chl-*a* trend was observed. In the English Channel, the shape of the seasonal cycle in Chl-*a* changed over time. Narrower peaks were observed in spring at the end of the studied period, indicating an earlier limitation by nutrients. Monthly averages of satellite Chl-*a*, over the periods 1998–2003 and 2012–2017, exhibited spatial and temporal patterns in the evolution of the phytoplankton biomass similar to these observed at the seven coastal stations. Both the *in situ* and satellite Chl-*a* times-series showed a decrease in Chl-*a* in the English Channel in May, June and July. This trend in phytoplankton biomass is correlated with lower river discharges at the end of the period and a constant reduction in the riverine input of phosphorus through improvements in the water quality of the surrounding river catchments.

1. Introduction

Coastal seas are highly productive regions that are subject to high anthropogenic nutrient inputs. The widespread use of fertilizers as a result of more intensive agricultural practices led to increased nutrient loads from the 1950s to the 1980s in European coastal waters (Vermaat et al., 2008). Due to the declining quality of these coastal waters, several European directives were enforced to improve the monitoring of

* Corresponding author.
E-mail address: Francis.Gohin@ifremer.fr (F. Gohin).

https://doi.org/10.1016/j.rse.2019.111343
Received 19 December 2018; Received in revised form 16 July 2019; Accepted 21 July 2019
Available online 12 September 2019

coastal waters. One of the major goals of water quality monitoring is an assessment of the effect of policy measures used to limit the nutrient enrichment, specifically phosphorus and nitrogen. Anthropogenic enrichment of the water column with these nutrients can cause an increase in the biomass of phytoplankton, resulting in a range of undesirable disturbances in the marine ecosystem. This is known as eutrophication. In 2000, the Water Framework Directive (WFD, 2000/60/EC) established a strategy to combat coastal pollution including those waters within one nautical mile from shore. Eutrophication has also been tackled by the recent European Marine Strategy Framework Directive (MSFD, 2008/56/EC) that aims to achieve Good Environmental Status (GES) of European Union (EU) marine waters by 2020. The GES means that marine resources are used at a sustainable level to ensure their continuity for future generations. To this end, the MSFD requires EU Members States to reduce nitrogen and phosphorus loads into the marine environment. Descriptor 5 of the Directive states that human-induced eutrophication should be minimized to reduce the loss of biodiversity and to prevent ecosystem degradation, harmful algae blooms and oxygen deficiency in bottom waters. The enrichment in nutrients by rivers in coastal waters is the cause of eutrophication that leads to elevated mean or 90th percentile of Chl-*a*. A statistical advantage of the 90th percentile is that it eliminates outliers frequently encountered in datasets of Chl-*a*. It is therefore a central parameter recommended for the assessment of the eutrophication status in the WFD, the MSFD (Ferreira et al., 2011) and in the North-East Atlantic environment strategy of the OSPAR commission (OSPAR Common procedure, 2013). All these water-quality monitoring systems cover wide maritime areas, which can only be observed through the use of remote-sensing data (Gohin et al., 2008; Novoa et al., 2012; Kratzer et al., 2014; Harvey et al., 2015). Remote-sensing products, Chl-*a*, turbidity, and phytoplankton type indicators have a considerable potential for enabling the convergence of the surveillance networks of the pelagic habitat requested by the different directives and regional conventions from coastal to open seas (Borja et al., 2010).

Since the launch of SeaWiFS in August 1997, followed by other sensors from NASA and ESA (European Space Agency), a continuous time series of satellite-derived Chl-*a* products is available for the monitoring of the marine environment. To assess the evolution of phytoplankton biomass over a twenty-year period (1998–2017) using both *in situ* and satellite data, the compatibility of the satellite-derived products with the conventional *in situ* retrievals has to be assessed. However, the performance assessment of ocean colour satellite data is a difficult task in absolute, particularly for the Chl-*a* non-gaussian distribution with outliers. It generally relies on mean squared errors, such as the coefficient of determination (r^2), root mean square error, and regression slopes. Seegers et al. (2018) discuss the limitations of these conventional methods and consider that end-user/application criteria should be determinant in the choice of the assessment metrics. The performance assessment of our satellite dataset will therefore be carried out on the 90th percentile calculated over the productive period (from the beginning of March to the end of October). This quantity is the key parameter of the Chl-*a* distribution involved in the water quality monitoring procedures already mentioned. In the field of eutrophication a specific attention is brought to high Chl-*a* values and the natural scale should be promoted in complement to the logarithm transformation of Chl-*a* usually proposed for assessing the quality of a satellite

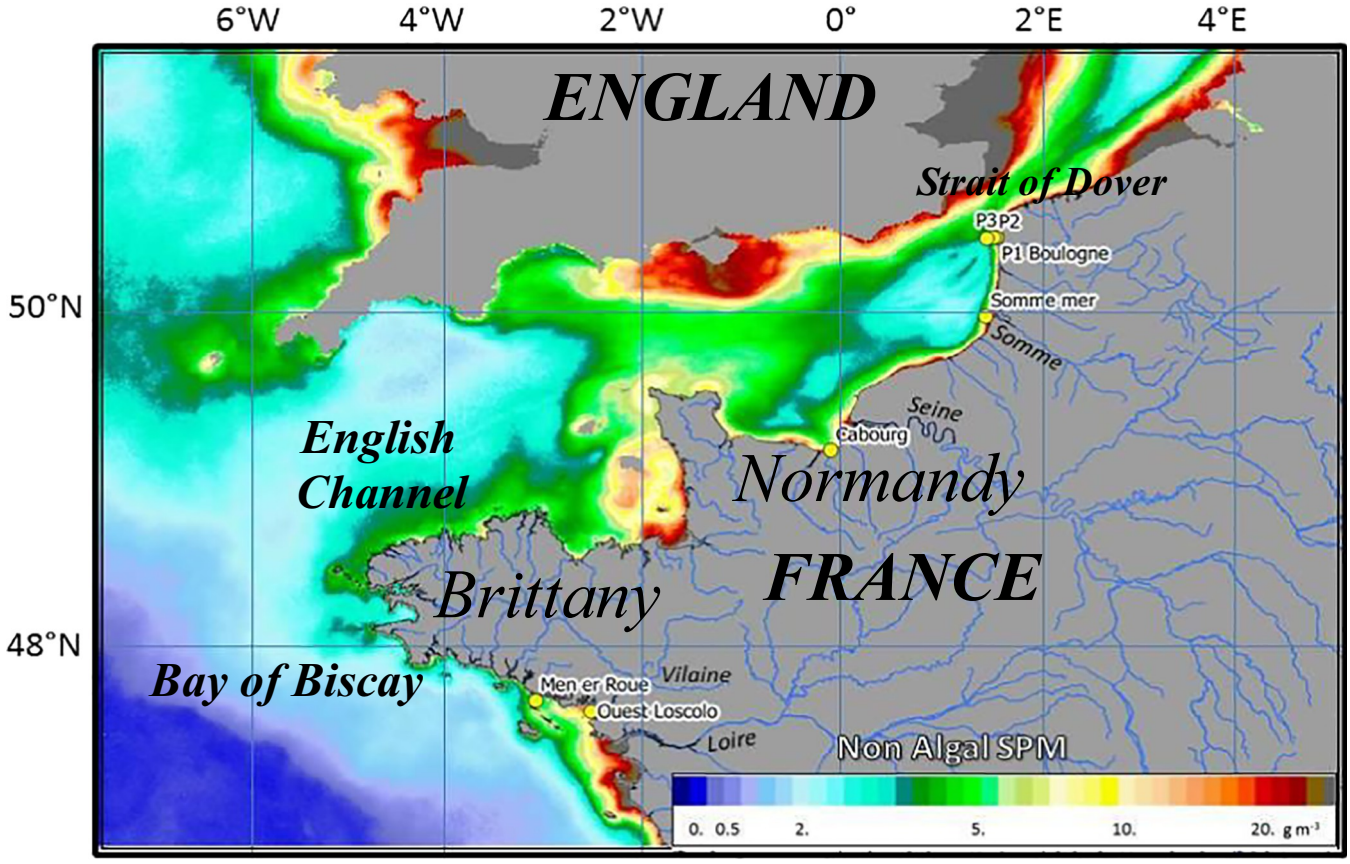

Fig. 1. Study area showing *in situ* station locations superimposed on averaged non-algal Suspended Particulate Matter at the end of winter (March) during the period 1998–2017. SPM is derived from satellite reflectance using the algorithm described in Gohin et al. (2005) and Jafar-Sidik et al. (2017).

product (Campbell et al., 1995). The priority is to provide from space accurate estimates of the elevated Chl-*a* concentrations encountered in case of massive phytoplankton blooms. The OC5 Ifremer (hereafter OC5) algorithm applied to marine reflectance in turbid waters (Gohin et al., 2002) is expected to perform well on a multi-sensor time series. OC5 is robust and provides relatively good retrievals of Chl-*a* compared to other algorithms, not just in north-west European coastal waters (Tilstone et al., 2017), but also in the western Mediterranean Sea (Lapucci et al., 2012; Gómez-Jakobsen et al., 2016), the coastal Vietnamese waters (Loisel et al., 2017), and at global scale (Saulquin et al., 2018). The OC5 Chl-a products that we propose to evaluate and use in this study are interpolated multi-sensor images obtained following the procedure proposed in Saulquin et al. (2011). These interpolated daily products can be recommended for operational monitoring of Chl-*a* and for providing monthly or yearly bulletins of anomalies based on well-balanced datasets in terms of spatial and temporal coverage (Leadbetter et al., 2018). The representativity of the annual cycle of satellite-derived Chl-*a*, compared to those observed *in situ*, has also to be assessed. Potential improvements in water quality should be observed in a lower 90th percentile of Chl-*a* and in a reduction of the growing period before limitation by nutrients. The annual cycles and the 90th percentile, assessed over years, are therefore the two properties of the Chl-*a* distribution recommended for assessing the performance of the satellite method in view of reporting on the eutrophication status for the European directives. Seven stations characteristic of coastal waters from the northern Bay of Biscay to the eastern English Channel have been selected for this assessment. Fig. 1 shows the location of the stations superimposed on the mean concentration of non-algal Suspended Particulate Matter (SPM) at the end of winter. All these stations are in nutrient-rich and moderately-turbid waters.

As the directives recommend a period of six years for the reporting of the monitoring programme, the average and the 90th percentile of Chl-*a* retrieved from space or observed *in situ* will be calculated also over this period. The main reason for this assessment period is that it gives time to assess the effect of measures or actions taken by the authorities in charge of the water quality in order to achieve or maintain good environmental status whilst being affordable in practice from *in situ* monitoring.

This 6-year average can also be applied to parameters that are potential drivers of the development of phytoplankton blooms arising from eutrophication. Based on *in situ* data, Capuzzo et al. (2018) identified the sea surface warming and reduced nutrient riverine inputs as the major causes in the decline of the primary productivity in the North-Sea over the period 1998–2013. A negative trend in the bloom intensity related to winter nutrients in the Baltic Sea over the period 2000–2014 was also observed by Groetsch et al. (2016). The variability and the trends in the discharge and the nutrients load (phosphorus and nitrate) of the main rivers running into the English Channel and the northern Bay of Biscay have to be investigated as the possible causes of the evolution of Chl-*a* observed on our twenty-year time series of satellite and *in situ* Chl-*a*.

2. Data and methods

2.1. The satellite dataset

The Chl-*a* concentrations were derived from the merging of SeaWiFS, MERIS, MODIS/AQUA and VIIRS remote-sensing reflectance processed by the coastal OC5 algorithm with Look-Up-Tables (LUT) dedicated to each sensor (Gohin et al., 2002; Gohin, 2011). The LUTs have been calibrated on the remote-sensing reflectance (Level 2 product) provided by the agencies in 2015 (2014 processing for MODIS and SeaWiFS; MEGS8.0 processing for MERIS). Since 2015, the MODIS and VIIRS reflectance data were those provided daily, by subscription,

Table 1
Locations and characteristics of the in-situ stations. Mean Chl-a and NTU are calculated over the productive season (March to October). >200 observations are available for each station over the period 1998–2017.

Station	Longitude	Latitude	Mean Chl-*a* (st.dev). mg m^{-3}	Mean turbidity (st.dev). NTU	Region	Particularity
Boulogne 1	1.55E	50.75 N	6.47 (5.1)	2.93 (2.5)	Eastern English Channel	Coastal on the Boulogne transect
Boulogne 2	1.52E	50.75 N	4.90 (5.28)	1.86 (1.42)	"	Mid
Boulogne 3	1.45E	50.75 N	2.87 (2.57)	1.13 (0.67)	"	Offshore
Somme_Mer	1.44E	50.23 N	7.69 (5.55)	2.24 (1.94)	Off the plume of the Somme river	
Cabourg (monitored since 2001)	O.12 W	49.30 N	17.74 (8.77)	3.02 (1.98)	Bay of Seine	The satellite location is one pixel (1.2 km) north off the station
Men er Roué	3.09 W	47.5 N	2.18 (2.34)	1.6 (1.62)	Bay of Biscay	Clear waters
Ouest_Loscolo	2.54 W	47.45 N	6.26 (7.59)	3.49 (3.74)	In the plume of the Vilaine river	Subject to eutrophication (anoxia) in summer

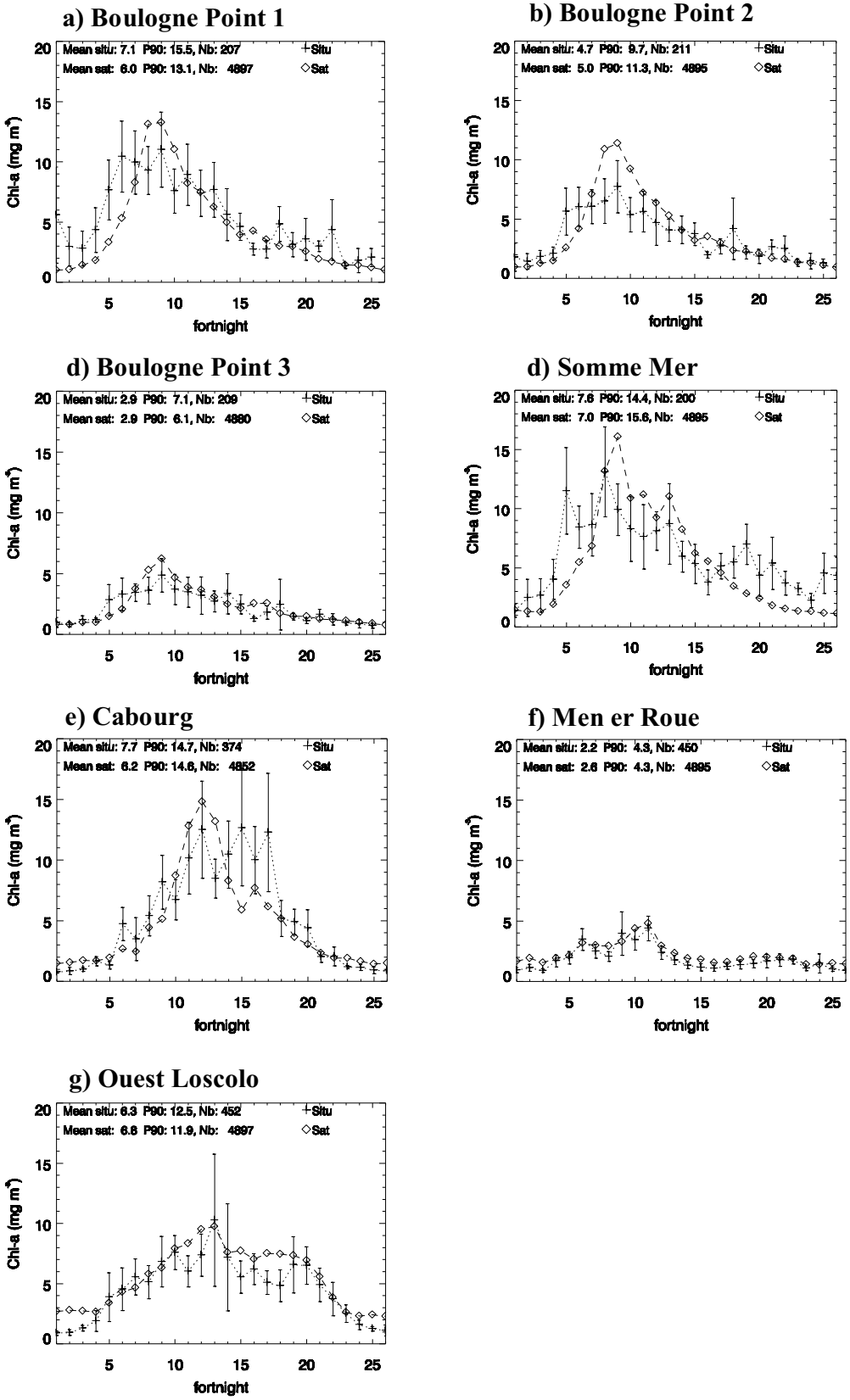

Fig. 2. The annual cycles of *in situ* and satellite Chl-*a* concentration at the selected stations. (a–c) the Boulogne transect; (d–e) the stations in the plumes of the Somme and Seine rivers: Somme_Mer and Cabourg. (f–g) stations in the Bay of Biscay. Means, 90th percentiles and number of data, indicated on the graphs, correspond to the productive period (March to October).

from the NASA Goddard Space flight Center. The OC5 algorithm used in that study is specifically designed for waters where suspended sediment may hamper the application of the classical OCx algorithms defined for the open ocean (O'Reilly et al., 1998; O'Reilly and Werdell, 2019). OC5 modifies the empirical relationships between *in situ* measurements of Chl-*a* and the blue-to-green ratios of the marine reflectance used as reference in the OC3 and OC4 algorithms, by including the radiances or reflectance at or near 412 and 555 nm from the level 2 satellite products provided by NASA or ESA. For high reflectance in the green waveband (555 nm), OC5 Chl-*a* tends to zero whereas it remains close to standard OC3 for MODIS and OC4 for SeaWiFS and MERIS in clear waters. In the OC5 LUT, the effect of SPM on the reflectance ratios used as inputs in OC3 and OC4 is revealed from the green channel at around 555 nm, whereas the atmospheric over-correction and the absorption by yellow substances are related to the blue channel at 412 nm (Gohin et al., 2002). The images used in this study are interpolated OC5 Chl-*a*, therefore a Level 4 product, following the nomenclature defined by NASA. The interpolation is performed using kriging techniques, which enable the creation of a daily multi-sensor dataset of complete images over the period 1998–2017 (ftp://ftp.ifremer.fr/ifremer/sextant-data/SATCOAST/atlantic/CHL, Ifremer, 2017). The spatial resolution of the interpolated images is 0.01° in latitude and 0.015° in longitude (about $1.2 * 1.2\,km^2$). In practice, the interpolation is carried out on Chl-a anomalies calculated by difference to a 1998–2008 daily average (SeaWiFS and MODIS/AQUA). Satellite data observed within 5 days before and 5 days after the day of interest and up to 160 km from the pixel location were used to build the data sets used for the daily interpolation. Despite possible artefacts on some images, the kriging estimator is unbiased and the interpolated Chl-a shows an excellent relationship with the *in-situ* observations in term of averages and 90th percentiles (Saulquin et al., 2011).

2.2. The in-situ datasets

The *in-situ* data of Chl-*a* (Fig. 1) were obtained from the "Suivi Régional des Nutriments" (SRN, 2017), the "Réseau Hydrologique Littoral Normand" (RHLN), and the Ifremer REPHY phytoplankton network (REPHY, 2017). Three stations (Boulogne 1, 2, 3) are located along a transect off the harbour of Boulogne. Somme_Mer is located in front of the mouth of the river Somme (mean annual discharge $35\,m^3\,s^{-1}$). The Boulogne and Somme_Mer stations belong to the SRN network with a monthly sampling frequency. The Cabourg station, belonging to the RHLN, is located in the vicinity of the Seine plume (mean annual discharge $510\,m^3\,s^{-1}$). The RHLN and REPHY networks have a 2-weekly sampling frequency. Two stations have been selected in the northern Bay of Biscay, Men er Roué in relatively clear waters and Ouest_Loscolo in the plume of the Vilaine river (mean annual discharge $70\,m^3\,s^{-1}$) in southern Brittany. The region under the influence of the Vilaine and the Loire rivers is subject to recurrent anoxia events in summer, favoured by high production and stratification (Chapelle et al., 1994). All stations have been sampled since 1998, except Cabourg where the sampling of the RHLN started in June 2001. Cabourg, Boulogne 1 and Ouest_Loscolo are located in the most eutrophic waters found in the English Channel and the Bay of Biscay. The Chl-*a* concentration was obtained mostly by monochromatic spectrometry following Aminot and Kérouel (2004) and Lorenzen (1967). More details on these stations and measurements, already used in Gohin (2011), can be found in REPHY (2017), SRN (2017) and Lefebvre et al. (2011). All these stations, except Cabourg, are at offshore locations where systematic failures in the atmospheric correction of the satellite reflectance do not occur. The comparisons are made at the station point locations with the exception of Cabourg where the satellite pixel is selected 0.01° (one pixel, *i.e.* 1.2 km) north of the coastal station. Locations and main characteristics of the stations are indicated on Table 1. Nitrate and phosphorus outflow data for the Seine and Vilaine rivers were obtained from "eaufrance", a public information system of aquatic environments in France. The outflows come from the "banque hydro" and the nutrients from the "naiades" website http://www.naiades.eaufrance.fr/acces-donnees#/physicochimie. For the Vilaine river, the outflows (2003–2017) and nutrients (1998–2017) are measured at Rieux. As the time series of the outflow of the Vilaine river is relatively short, we also used the outflows of the Loire river at Monjean-sur-Loire (mean annual discharge $843\,m^3\,s^{-1}$) that are highly correlated to those of the Vilaine river. For the Seine river, measurements (1998–2017) are carried out at the dam of Poses.

3. Results

3.1. The annual cycles at the stations

Fig. 2 shows the annual cycles of satellite and *in situ* Chl-*a* at the seven sampling stations as well as the mean and the 90th percentile over the productive period. Despite the fact that the satellite data are interpolated, the level and shape of the curves are very similar to those obtained from mono-sensor (non-interpolated) data (Gohin, 2011). Such a result was expected, since the kriging method used for the interpolation is unbiased. The major discrepancy between the satellite and *in situ* data sets is observed in winter along the cross-shore transect off Boulogne. High Chl-*a* concentrations are observed *in situ* very early in the year, even in January. Nevertheless, both SRN and satellite data sets illustrate that the phytoplankton development starts early in the Northern English Channel (as in the North-Sea), though the satellite Chl-*a* is lower. The stations in the river plumes, Somme_Mer, Cabourg and Ouest-Loscolo, exhibit bell curves typical of eutrophic waters enriched by a constant flux of riverine nutrients. Despite some differences between the datasets, the means and 90th percentile of Chl-*a* are very similar. The correspondence is high between the satellite-derived and *in situ* gradients along the Boulogne transect; with mean levels over the productive period of about 6, 5 and $3\,\mu g\,m^{-3}$ from coastal (Point 1) to deeper waters (Point 2 and 3).

3.2. The temporal evolution in Chl-a at the stations

3.2.1. Evolution of the yearly means with time

Fig. 3 gives the yearly means for the productive season (March–-October) at the selected stations. The vertical bars around the *in situ* averages correspond to approximate confidence intervals on the mean at 90% ($\pm 1.65\sqrt{s^2/n}$ where s^2 is the standard deviation and n the number of data) for a Gaussian distribution, indicative of the variability in the *in situ* data. Such a representation is not applicable to the satellite data as these are so numerous (204 retrievals each year within the productive period) that their average is a very accurate estimation of their statistical mean. Thus, the weakness of the satellite averages could concern more the bias that they can show with the *in-situ* reference than their variance. That is why it has been so important to roughly assess this bias locally and seasonally by comparing the mean annual curves of satellite and *in situ* Chl-*a* and their major statistics (Fig. 2). Despite a high variability of the *in-situ* measurements, as at the Ouest_Loscolo station in 2007 with two outliers observed at 115 and $75\,mg\,m^{-3}$, the time-series of the yearly means derived from the satellite or observed at sea show similar dynamics over years.

The time-series of the six-year moving averages (Fig. 4) and 90th percentiles (Fig. 5) show a decrease at the stations in the English

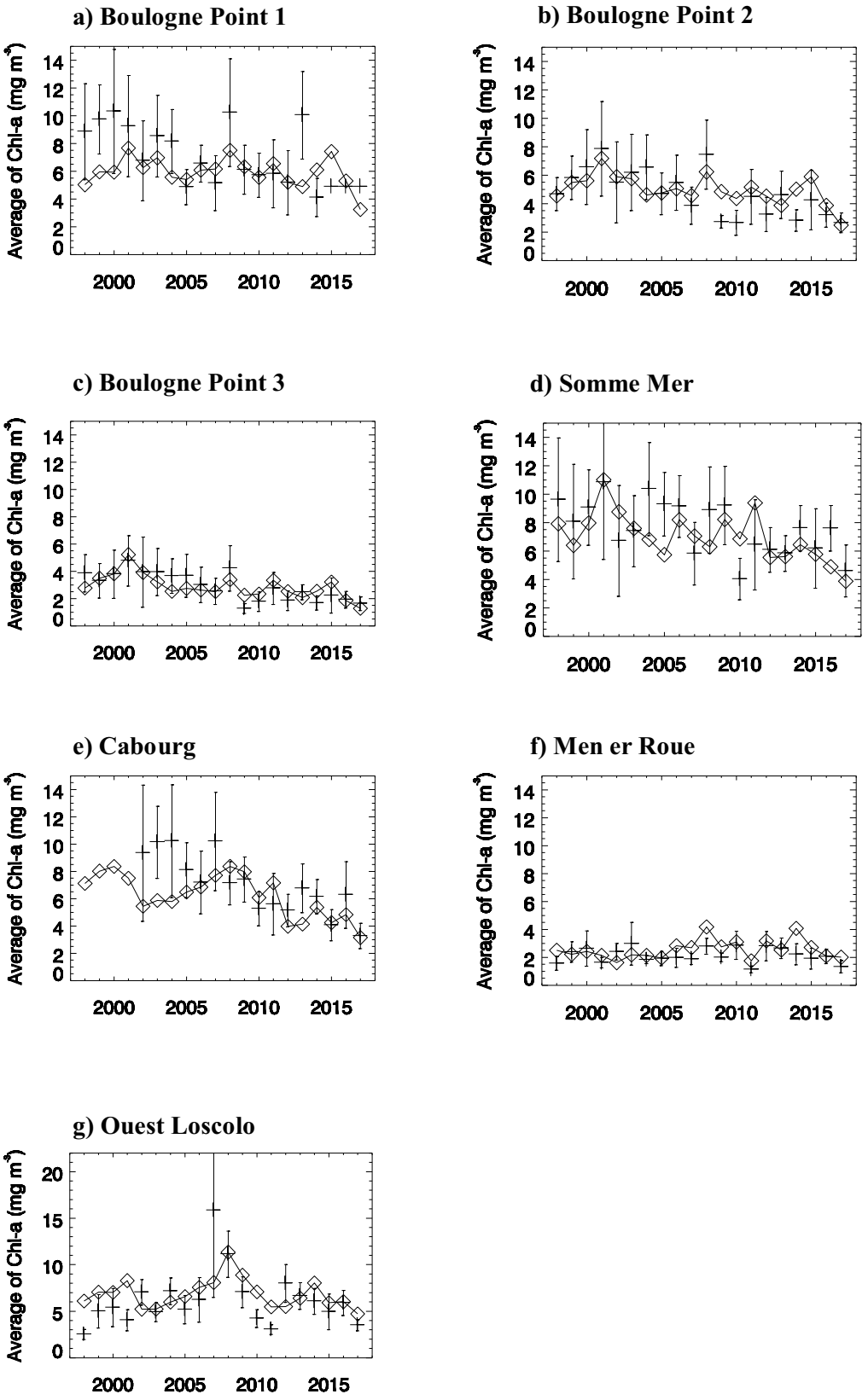

Fig. 3. The yearly average of the *in situ* and satellite (continuous line) Chl-*a* concentration at the selected station during the productive season (March to September). (a–c) the Boulogne transect; (d–e) the stations in the plumes of the Somme and Seine rivers: Somme_Mer and Cabourg. (f–g) stations in the Bay of Biscay. Bars around the in situ means correspond to 1.65* their standard error.

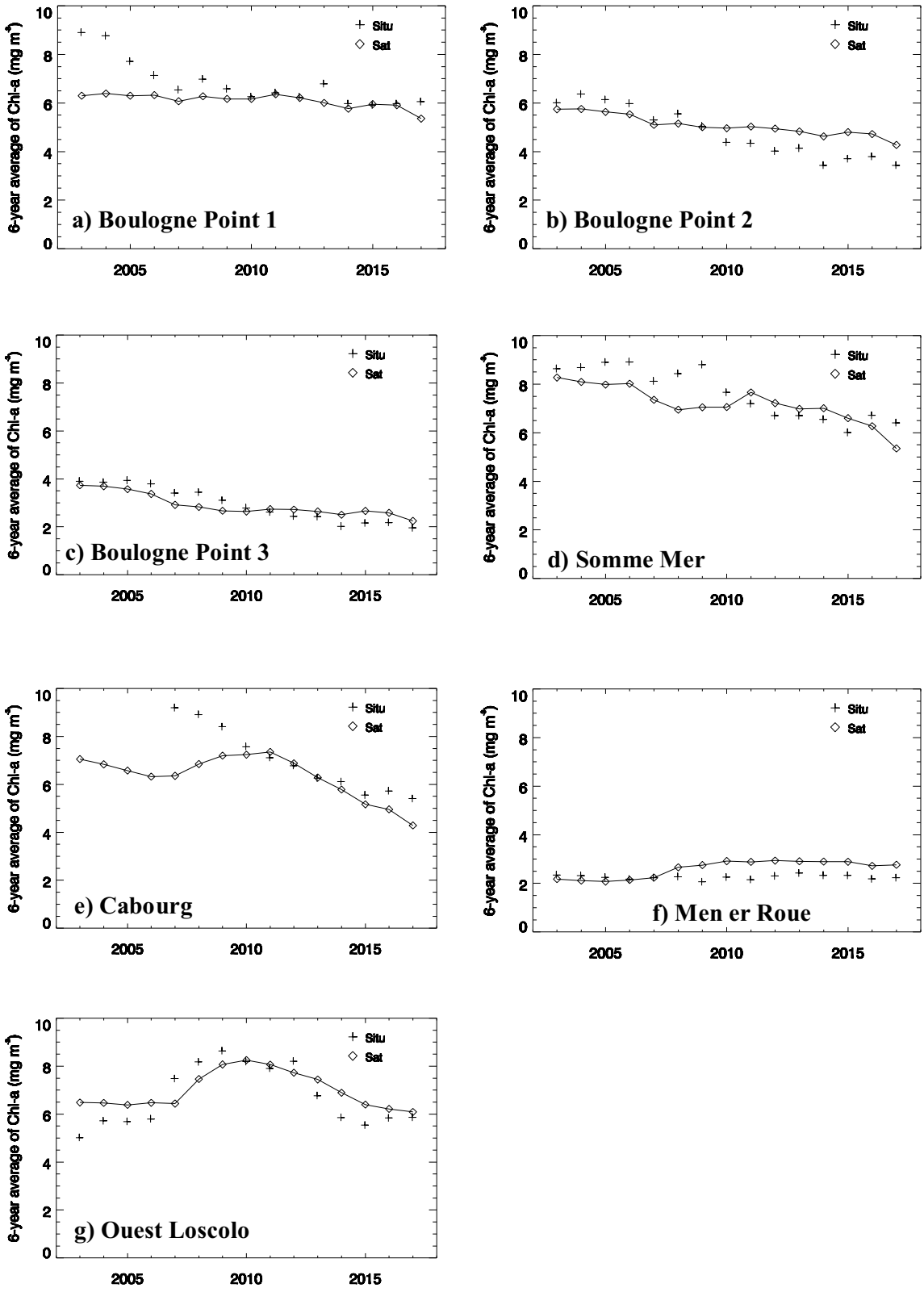

Fig. 4. The 6-year moving average of the *in situ* and satellite (continuous line) Chl-a concentration at the selected stations. (a–c) the Boulogne transect; (d–e) the stations in the plumes of the Somme and Seine rivers: Somme_Mer and Cabourg. (f–g) stations in the Bay of Biscay. The average is calculated over the productive season (March to October).

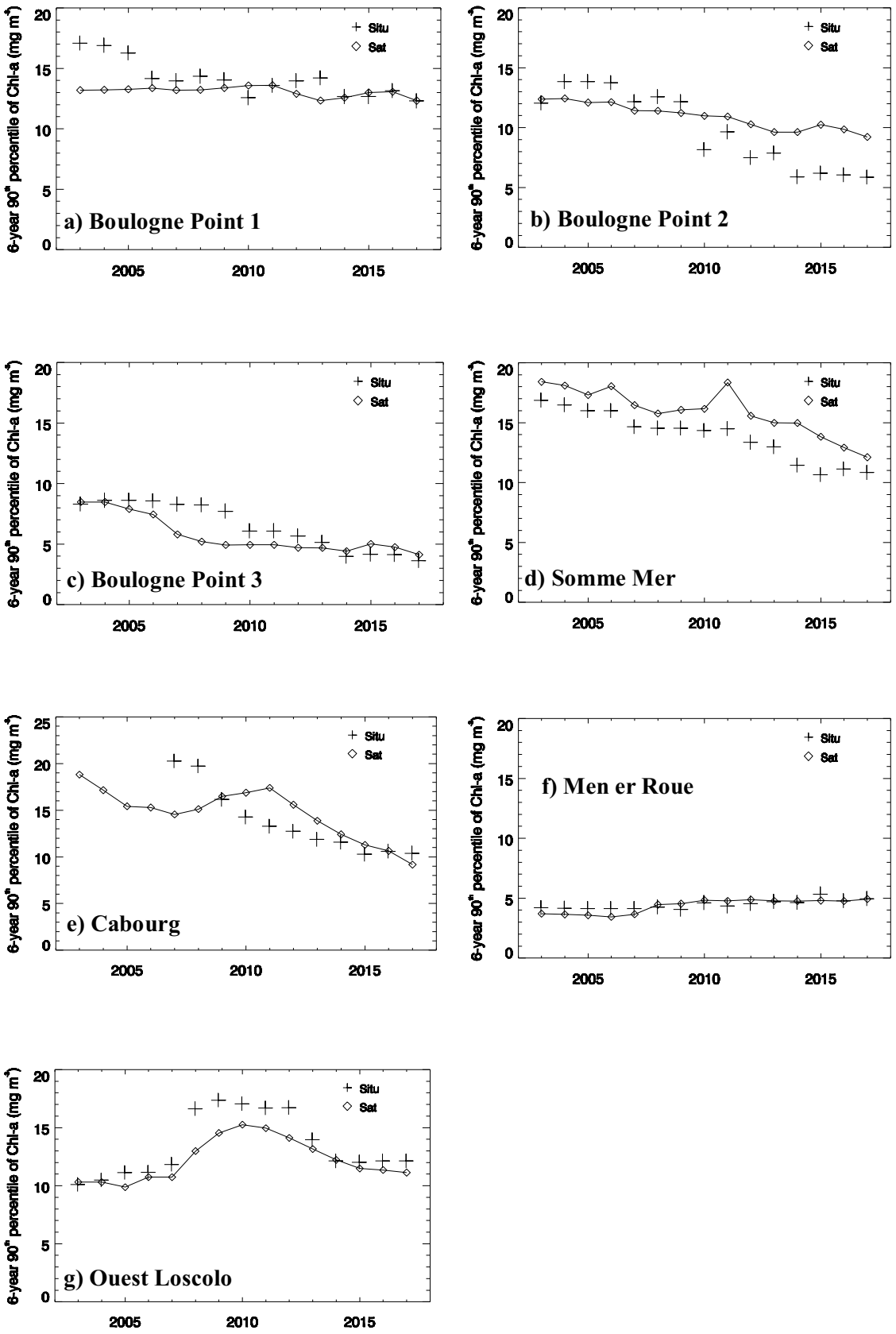

Fig. 5. The 6-year moving 90th percentile of the *in situ* and satellite (continuous line) Chl-*a* concentration at the selected stations. (a–c) the Boulogne transect; (d–e) the stations in the plumes of the Somme and Seine rivers: Somme_Mer and Cabourg. (f–g) stations in the Bay of Biscay. The 90th percentile is calculated over the productive season (March to October).

Channel whereas no significant trend is observed in the Bay of Biscay (stations Men er Roue and Ouest_Loscolo). Fig. 6 presents the 90th percentiles of Chl-*a* at the beginning (1998–2003) and at the end of the period (2012–2017) over the area. These maps show that the Men er Roue and Ouest-Loscolo stations are very representative of the Bay of Biscay characterised by an absence of long term trend in the 90th percentile of Chl-*a*, which contrasts with the southern coast of the English Channel and the southern bight of the North-Sea.

3.2.2. Temporal evolution of the annual cycle

If we restrict our samples to periods of 6 years, the lack of *in situ* observations makes the representation of the annual cycle from this data source less reliable. However, in parallel with lower averages, the shape of the Chl-*a* curve retrieved from satellite and *in situ* data clearly

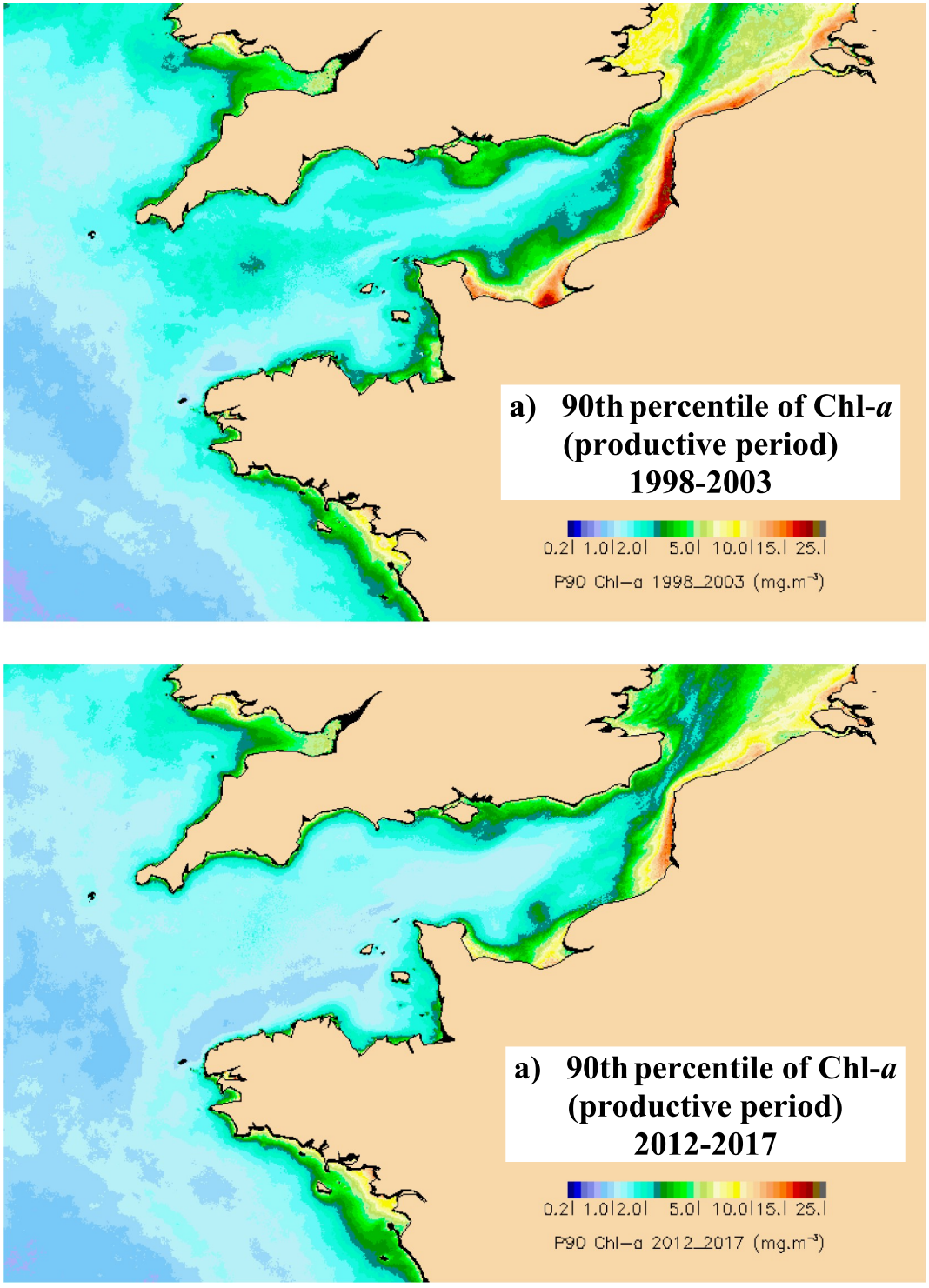

Fig. 6. The 90th percentile of Chl-*a* at the beginning and at the end of the studied period. (a) 1998–2003; (b) 2012–2017.

shows an evolution towards those of oceanic regions characterised by a spring peak followed by lower Chl-*a* concentration in nutrient-deprived waters. Fig. 7 shows the evolution from a "bell shape" to a "peak shape" at the Boulogne Point 2. In 2004–2011 and 2012–2017, the annual cycles of Chl-a show a "peak shape" and are characterised by a decrease in Chl-*a* at fortnightly intervals from 10 to 15 (May to July), whereas in 1998–2003 Chl-*a* is still high at this period. The decrease in Chl-*a* observed at the last period, 2012–2017, is accentuated in the *in-situ* data set by the small number of observations available (73 for the productive period).

Fig. 8 shows typical curves during years of high Chl-*a* (2001 and 2008) compared to years exhibiting lower Chl-*a* (2016 and 2017).

To investigate the phytoplankton dynamics throughout the seasons, the satellite data provide more spatial and temporal coverage as illustrated in Fig. 9, which shows the monthly means of Chl-*a* at the beginning and the end of the study period. During March and April, Chl-*a* is similar for both periods, whilst May and June exhibit a clear decline in Chl-*a* in the southern English Channel.

4. Discussion

4.1. Regional evolution of the phytoplankton biomass

The evolution of Chl-*a* can be analysed at point scale using *in situ* data or at regional scale using satellite data. The deviation between *in situ* and satellite data shown in Figs. 4 and 5 is enhanced at near-shore coastal stations where patterns of Chl-*a* may exist at a range unreachable at the current 1 km resolution of satellite sensors. The Boulogne Point 1 and Cabourg stations are the most in shore stations and exhibit the highest discrepancy between satellite and *in situ* observations (Figs. 4a and e, 5a and e). This deviation could come from the remote-sensing technique itself, as particularly complex optical properties and environment effects, due to the influence of neighbouring land pixels, could affect the quality of the atmospheric correction in waters near the shore. Another plausible explanation is that there has been a substantial improvement in the waste water treatment from neighbouring cities (after application of measures requested by the EU directive on the bathing water quality) since the end of the 1990's, leading to lower nutrient input from sewage effluent into near-shore coastal waters. This may have had strong influence at the Cabourg station which is so close to the coast that, in order to obtain satellite data that are not flagged as land, the location of the pixel was shifted one kilometre northward. There are indeed two scales in the evolution of the nutrient fluxes that affect the coastal waters; one occurs at very short range due to specific improvement locally, in bathing water quality, and the second occurs over a larger regional level, which is related to the evolution of the inputs from major rivers, such as the Seine, Loire, Somme and Vilaine rivers which affect the entire area.

At a regional level, there are three main areas that exhibit specific and characteristic trends in remote-sensing Chl-*a*: the southern Brittany in the Bay of Biscay, the western English Channel, and the "Fleuve côtier"; the Region Of Freshwater Influence (ROFI) from the Bay of Seine to the Strait of Dover in the eastern English Channel (Brylinski and Lagadeuc, 1990; Brylinski et al., 1991) with influence farther north

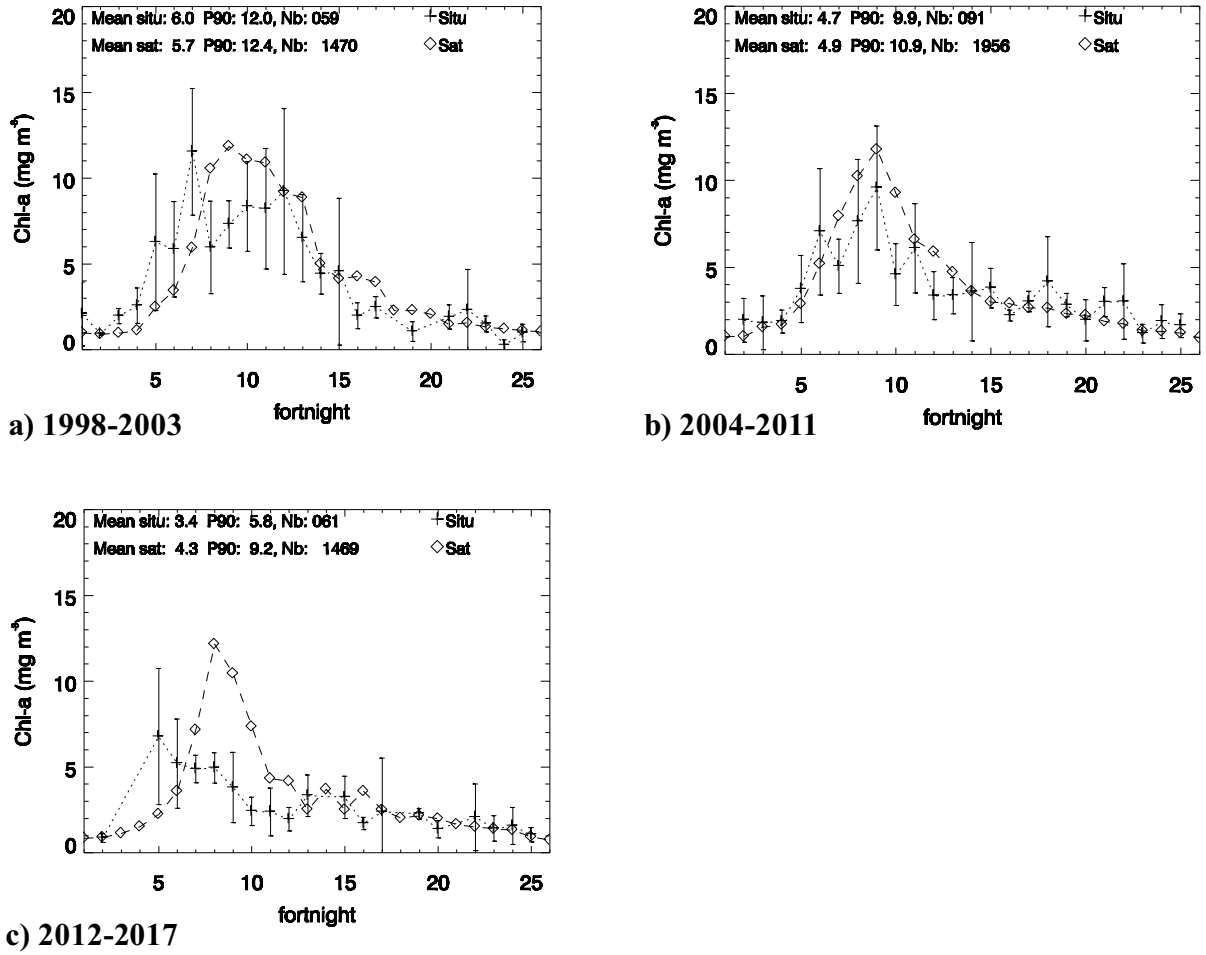

Fig. 7. Evolution of the seasonal cycle of Chl-*a* at Boulogne Point 2 over the 1998–2017 period. (a) 1998–2003; (b) 2004–2011; (c) 2012–2017 The averages (satellite and *in situ*) indicated on the graphs are calculated over the productive season.

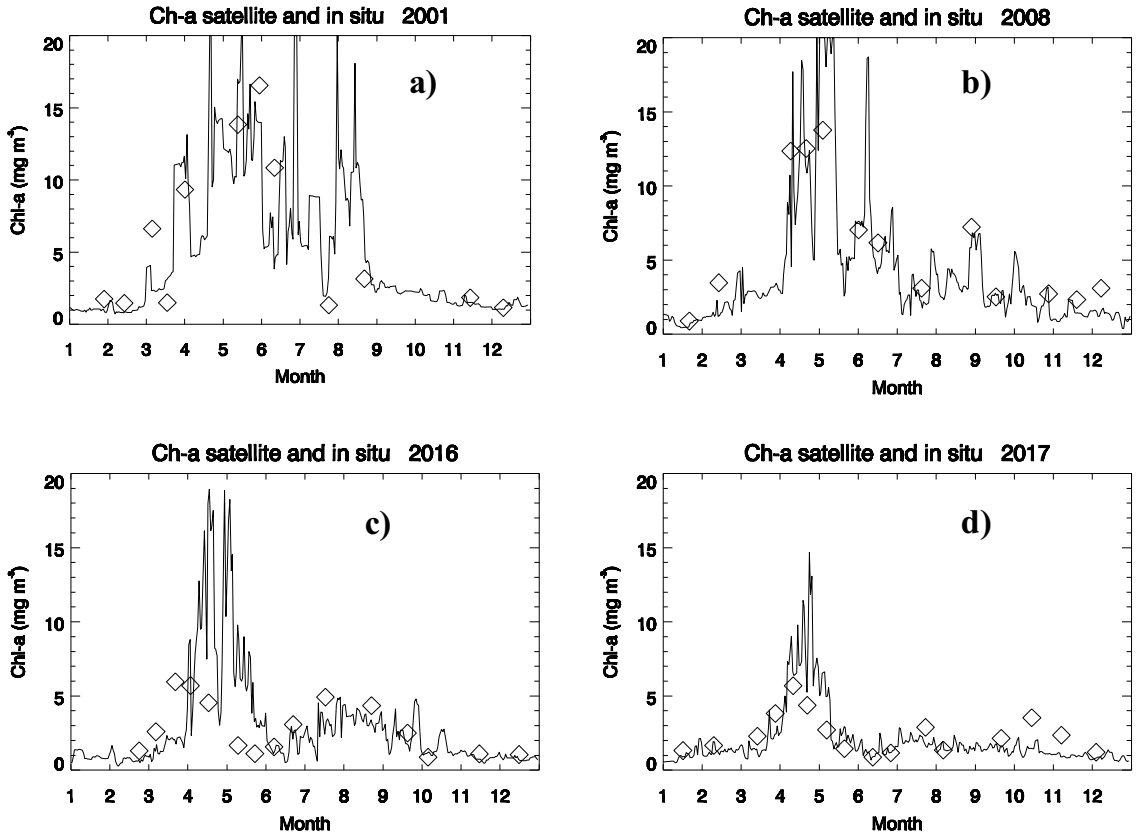

Fig. 8. Typical Chl-*a* cycles at Boulogne Point 2. (a) 2001 and (b) 2008 high Chl-*a* years; (c) 2016 and (d) 2017 low Chl-*a* years. Diamonds: *in situ* data; continuous line: satellite data.

in the southern North-Sea (Lacroix et al., 2007).

It is in this latter region that the evolution of Chl-*a* is the strongest. The "Fleuve Côtier" exhibits a lower signature in Chl-*a* in the period 2012–2017 compared to 1998–2003 (Fig. 6) along the coast, from its source, the river Seine, to the Dover Strait. The decrease in Chl-*a* is the most significant in the Bay of Seine, especially from May to July. In the north, the spring peak is as strong as ever in April. During April, *Phaeocystis globosa* blooms in high biomass, when it can form large gelatinous colonies that can impact benthic and pelagic ecosystems, and have been identified from the Somme river to the Southern North-Sea (Lancelot et al., 2014). The nutrient cycle in this region follows a typical temperate cycle, accumulating in winter and decreasing through phytoplankton uptake in spring (Lefebvre et al., 2011). After the diatom bloom that occurs from February to mid-April, the reduction in silicate and phosphate concentrations gives a competitive advantage to the small cells of *Phaeocystis globosa*.

Along the southern Brittany coast, there is no significant trend in the pattern and level of Chl-*a* from the beginning to the end of the study period. At the end of the period, the risk of eutrophication remains high in summer when waters stratify and high temperatures lower the concentration of dissolved oxygen.

The western English Channel, particularly the frontal zone between the summer stratified waters of the Atlantic Ocean and the mixed waters of the central English Channel, also has significantly lower levels of phytoplankton biomass at the end of the period. This area where high blooms of the harmful species *Karenia mikimotoi* may occur (Vanhoutte-Brunier et al., 2008) is under the influence of the north-Atlantic hydroclimate and of the inputs in fresh water and nutrients from the rivers flowing into the Bay of Biscay. The evolution of the satellite average of Chl-*a* in July between the periods 1998–2003 and 2012–2017 is also exacerbated by the conjunction of a major heat wave in 2003 that enhanced frontal patterns in the western English Channel and relatively higher fluxes of nutrients from the rivers flowing into the Bay of Biscay.

4.2. How do the rivers determine the surface Chl-a in the English Channel and the northern Bay of Biscay?

As any other marine environment, the coastal system of western Europe is driven by climate (Goberville et al., 2010), through the North Atlantic Oscillation (NAO) and the Atlantic Multidecadal Oscillation (AMO), with effects on the river outflows, the inputs in nutrients, the solar irradiance and the sea surface temperature that impacts stratification. Despite the fact that sea surface temperature is increasing in the eastern English Channel and in the North-Sea (Saulquin and Gohin, 2010), this warming cannot be the dominant factor in the evolution of the phytoplankton biomass at our *in situ* stations under the influence of highly variable freshwater fluxes. River discharges have evolved quantitatively through the period 1998–2017, in relation to precipitation in the watersheds; which have also undergone a significant qualitative change through a considerable decrease in phosphorus (Romero et al., 2013).

4.2.1. The influence of the Seine river on the evolution of the Chl-a in the English Channel

Fig. 10a–c, shows the outflows and the averages in nitrate and phosphorus in the Seine river processed over a 6-year period during the productive season. This is similar to the observations of Romero et al. (2013) who studied the Bay of Seine from 2000 to 2010, and observed that the nitrogen load remained high whilst phosphorus decreased dramatically. Using 17 stations from the RHLN Networks in the Bay of Seine from 2000 to 2010 (including the Cabourg station that is particularly well sampled) Romero et al., 2013 also observed a significant decrease in Chl-*a*, which we also observed from 2011 to 2017. Higher discharge (Fig. 10a) from the Seine river from 1998 to 2003

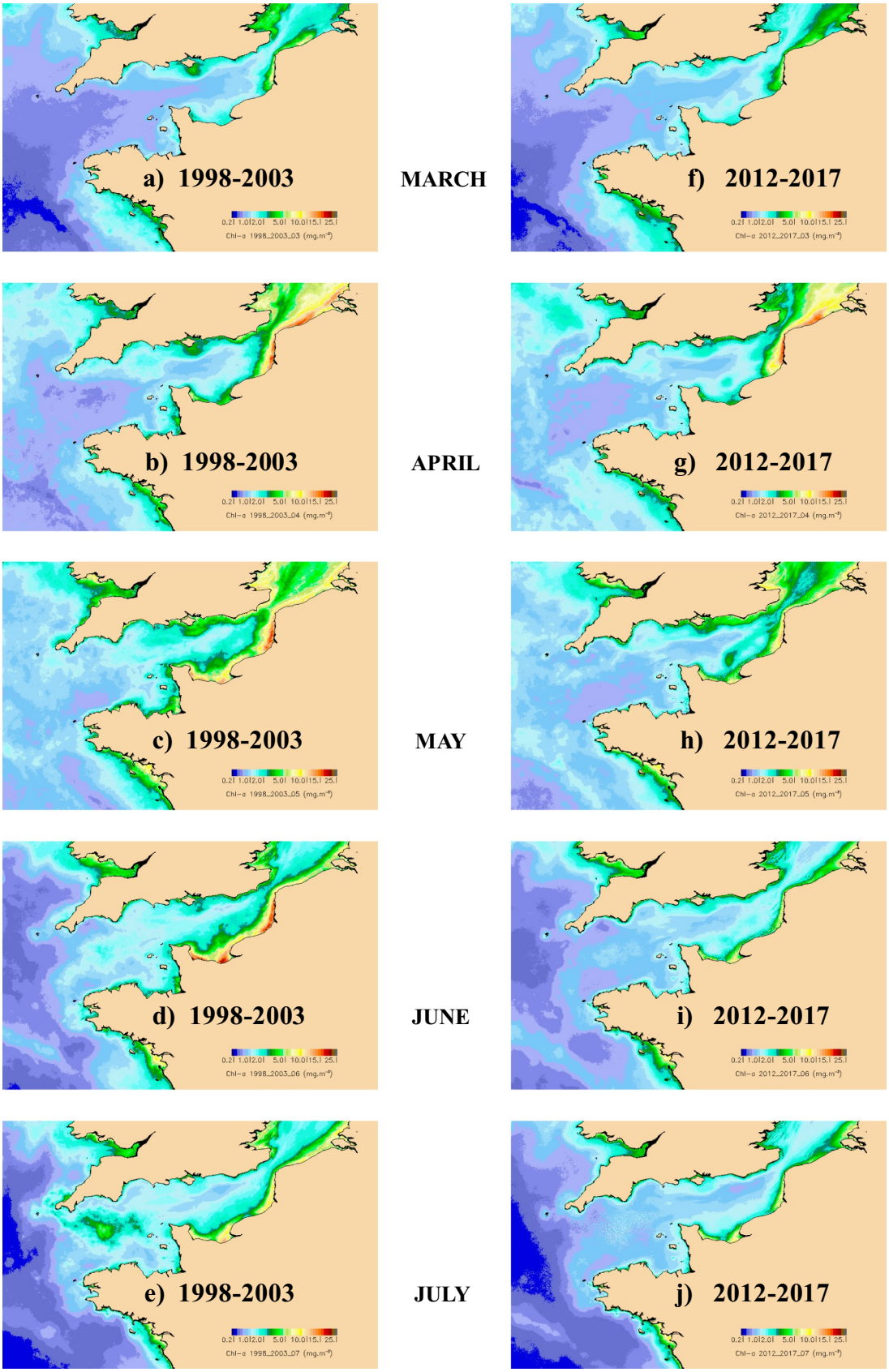

Fig. 9. Monthly means of the Chl-*a* concentration. (a–e) 1998–2003; (f–j) 2012–2017.

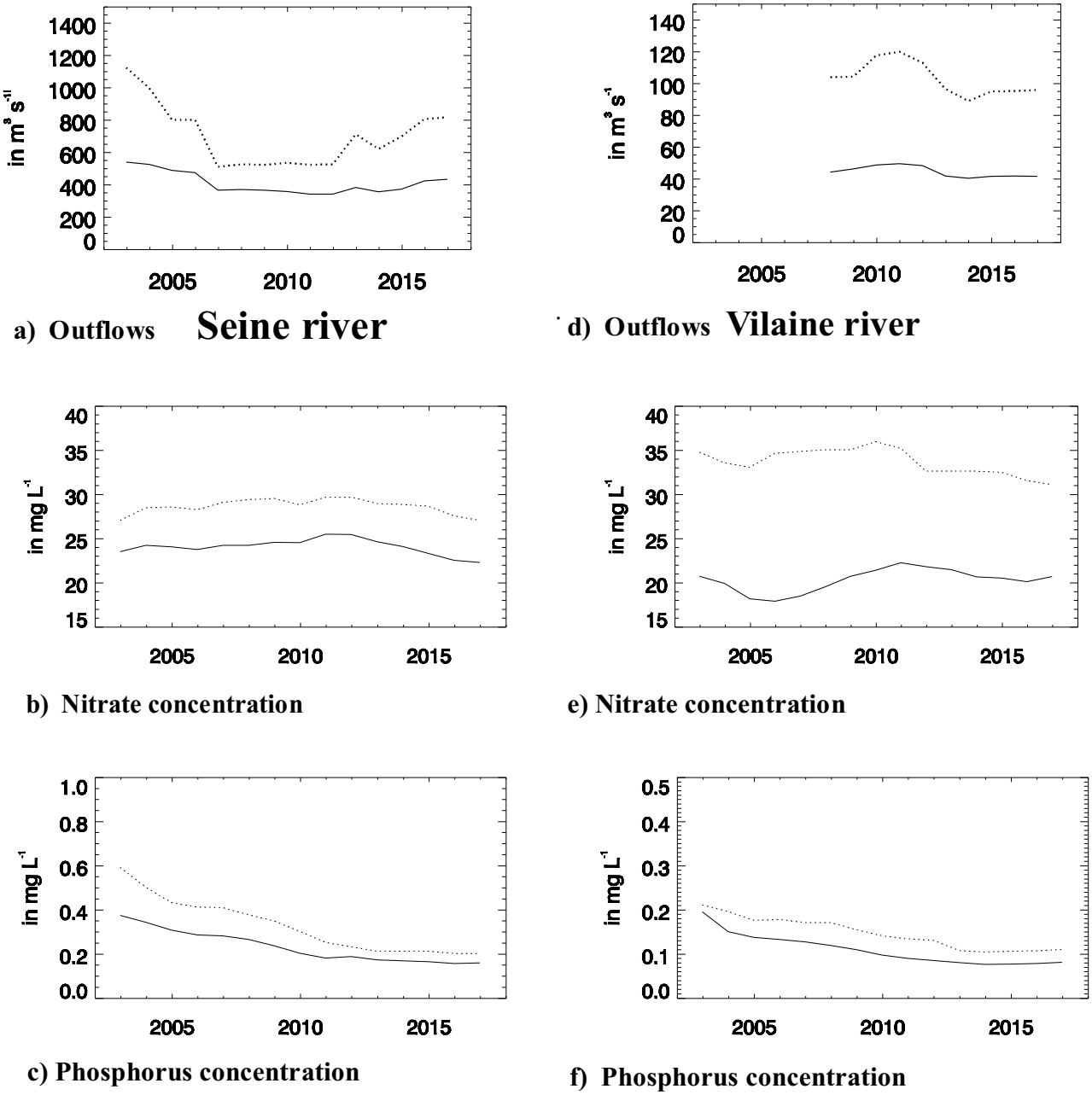

Fig. 10. Outflows, nitrate and phosphorus concentration during the productive season for the Seine and Vilaine rivers. (a–c) Seine river; (d–f) Vilaine river. The moving average and the 90th percentile are indicated in continuous and dotted line respectively.

(particularly winters 2000 and 2001) contributed to the negative trend in Chl-*a* observed over the period 1998–2017. Fig. 11 indicates that at the Boulogne 3 station, though furthest from the mouth of the Seine river, the effect of the discharge from the Seine is still strong. Lower outflows from the Seine river are associated with higher salinity at Boulogne Point 3, confirming the role of the "Fleuve côtier" in carrying fresh water from the Seine and Somme rivers northward (Brylinski et al., 1991). Higher river outflows (*e.g.* Seine, Somme, …), associated with higher N fluxes to these coastal waters (Passy et al., 2013), could drive the productivity of the eastern English Channel waters, mainly under N-limitation. The relative decrease in the Seine's discharges explained the trend in Chl-*a* though there was a recovery in the outflow after 2012 (Fig. 11) which doesn't show the expected effect, supporting the hypothesis of a possible limitation by phosphorus (Romero et al., 2013). The steady decline at Somme_Mer, both in the mean and 90th percentile of Chl-*a* (Figs. 4 and 5), might be also related to the drop in phosphorus from the rivers. Discharge data collected at Abbeville, along the Somme river, since 2006 showed an increase in the last years, similarly to the Seine's discharges, without changing the negative trend in Chl-*a*.

4.2.2. The influence of the Loire and Vilaine rivers on the evolution of the Chl-a in the Northern Bay of Biscay

By contrast to the English Channel, the Chl-*a* time-series observed from space and *in situ* at Ouest_Loscolo and Men er Roue do not show any significant trend over the studied period despite a decline in phosphorus similar to that observed in the English Channel (Fig. 10f). At the Ouest_Loscolo station, the average and 90th percentile of Chl-*a*

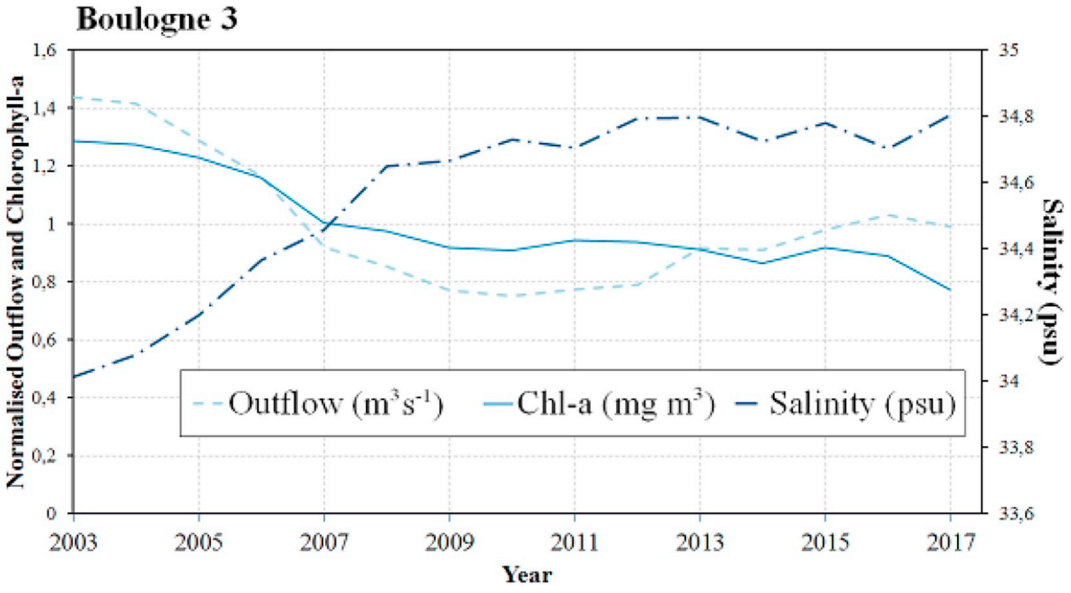

Fig. 11. Evolution of the 6-year average of the *in situ* Chl-*a* (productive period) versus the salinity at Boulogne Point 3 and the outflow of the Seine river (March to April) over the period 1998–2017. Chl-*a* and outflow are normalized by their means (2.9 g m^{-3} and 693 $m^3 s^{-1}$ respectively).

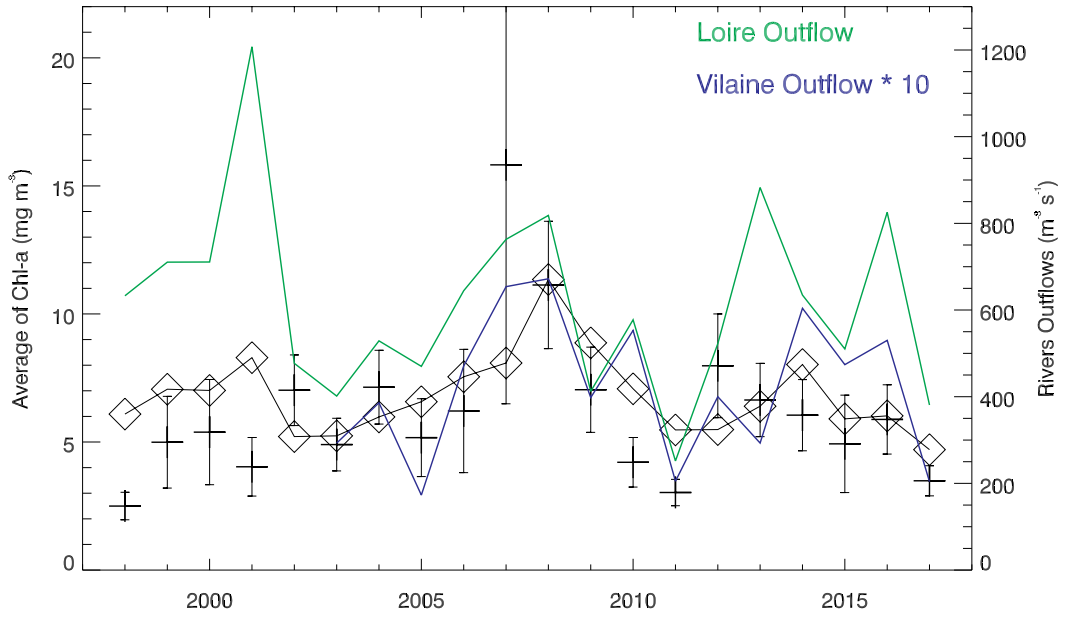

Fig. 12. The averaged satellite (black line and diamonds) and *in situ* (crosses) Chl-*a* during the productive season at Ouest_Loscolo in the Vilaine Bay compared to the averaged outflows of the Loire (green) and Vilaine (blue) rivers. The outflows of the Vilaine river are multiplied by 10. (For interpretation of the references to colour in this figure legend, the reader is referred to the web version of this article.)

appear to be clearly correlated with the river outflows over the productive period (Fig. 12), corroborating the results of Ratmaya et al. (2019). Fig. 13 shows that the sensitivity of the 90th percentile of Chl-*a* to the river outflow is also observed over a large part of the continental shelf.

4.3. How does a decrease in phosphorus affect phytoplankton diversity and harmful algal blooms (HABs) in the region?

Over the last few decades, a more effective reduction in loads of P relative to N has been observed in western Europe (Romero et al., 2013). Imbalanced inputs of N and P to coastal ecosystems can shift the stoichiometry of nutrients away from the Redfield ratio, which can in turn affect ecosystem characteristics such as nutrient limitation, turnover, and ultimately ecosystem productivity. Since certain phytoplankton species are expected to dominate at their optimal resource ratio, changes in nutrient stoichiometry may also lead to a modification of the composition of phytoplankton assemblages (Tilman, 1982). For example high N:Si or N:P ratios correspond to the initiation of *Phaeocystis* spp. blooms along the eastern English Channel (Karasiewicz et al., 2018). In spite of the reduction in P loads, sustained high values of N still foster the emergence of *Phaeocystis* spp. and other HABs, as expected by Romero et al. (2013). Over the period 2012–2017, despite a lower concentration of Chl-*a*, *Phaeocystis* counts remain high along the

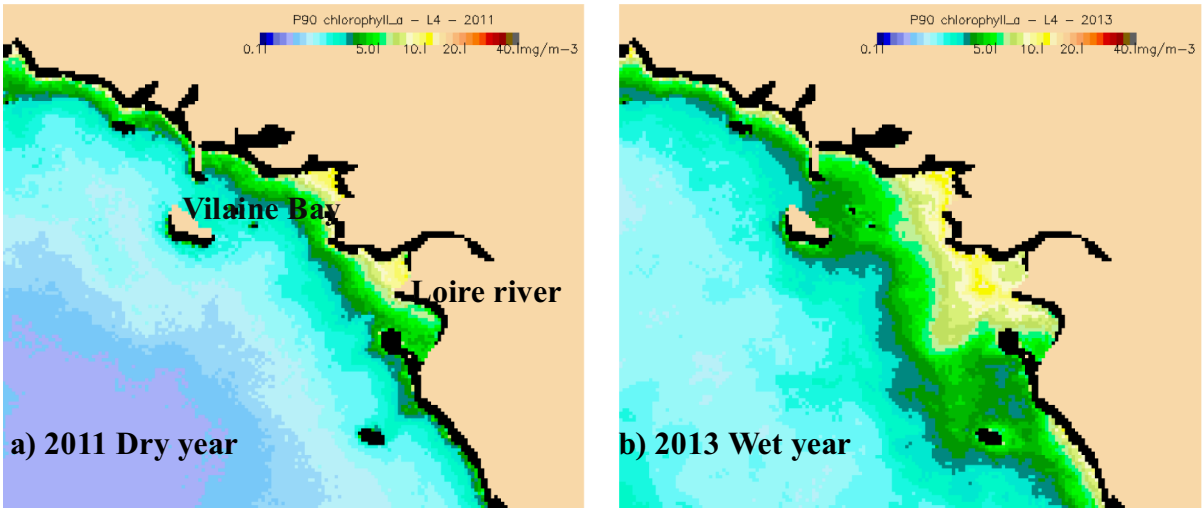

Fig. 13. 90th Percentile of Chl-*a* (productive season) in southern Brittany corresponding to two contrasting years: a) 2011 (dry) and b) 2013 (wet).

Boulogne transect, frequently reaching 3.5 10^6 cells L^{-1} in April.

Further research to assess the consequences of lower phosphorus export by the rivers should combine Chl-*a* with abundance and composition indicators. A change in phytoplankton biomass (positive or negative), can result in a shift, from diatom-dominated to a flagellates or *Phaeocystis* sp. dominated community, which would impact the structure and function of the benthic and pelagic ecosystems (*e.g.* Hernández Fariñas et al., 2014; Karasiewicz et al., 2018). Whilst the total phytoplankton biomass may not decrease, phytoplankton community composition may change favouring smaller cells, mixotrophs and motile species. Ecosystems are able to change their functional strategies as resource availability changes (Wentzky et al., 2018).

4.4. Consequence on the environmental status?

Measuring phytoplankton biodiversity, community composition, biomass and the frequency of HABs and associated variables over a sustained and long term basis is of primary importance to assess ecosystem status and trends in the coastal environment. Due to its high sensitivity to the changing environment globally, and its high reactivity to short term events (local pressures from anthropogenic sources), phytoplankton is a core indicator for Directives and Regional Sea Conventions for eutrophication and biodiversity assessments. Our results have major implications for several key descriptors of the environment of the coastal shelf monitored by the MSFD. Descriptor 1 (Pelagic Habitats), Descriptor 4 (a food web ensuring long term abundance) and Descriptor 5 (eutrophication) specifically could be affected by a decrease in Chl-*a* concentration. Descriptors 1 and 4 may be affected negatively and Descriptor 5 may be affected positively in the English Channel (not in the Bay of Biscay) since our results reflect a decrease in elevated chlorophyll-a events.

This trend in Chl-*a* could have a potential negative impact on the food chain and particularly on the growth of bivalves. By contrast, Bryère et al. (2019) did not observe a significant effect of lower Chl-*a* concentrations on the production of mussels at the end of the 1998–2018 period in western Europe using a dynamic energy budget model (Thomas et al., 2011) forced with CMEMS Chl-*a* also derived from the OC5 method. The main reason is that the decrease in Chl-*a* impacts mostly elevated concentrations ($>10\,mg\,m^{-3}$), far higher than the optimal level ($<2\,mg\,m^{-3}$) required for the growth of mussels. These results show also that this decrease in phytoplankton biomass has probably only minor effects on the overall quality of the phytoplankton as a component of the diverse descriptors contributing to the definition of the Good Environment Status, *e.g.* biodiversity, food web, … whereas the eutrophication risk, derived from the 90th percentile of Chl-*a*, decreases in the English Channel, despite a persistence of the HAB-forming *Phaeocystis globosa*.

Further work should assess the relative contribution of climate change effects *versus* the riverine inflow of nutrients in the evolution of the phytoplankton biomass in the frontal area between the stratified Atlantic Ocean and the mixed waters of the central English Channel. This is where remote sensing is of particular importance since the spatial scales of the marine processes involved over the continental shelf can vary from hundreds of meters from the shore to hundreds of kilometres in the open ocean.

4.5. Satellite algorithms and Chl-a products for north-west European waters and the limitations of OC5

The multi-sensor satellite Chl-*a* products presented here were generated with the OC5 algorithm which is optimized for the English Channel and the Bay of Biscay where different types of water are encountered, from clear (*i.e.* case 1) to moderately turbid (*i.e.* case 2). In very clear waters, when Chl-*a* concentrations are $<0.2\,mg\,m^{-3}$, OC5 has similar limitations to the OCx algorithms. Other algorithms, such as the Colour Index CI (Hu et al., 2012), may be preferable. In more extreme conditions, in terms of SPM and CDOM but also when the Chl-*a* concentration increases to high levels ($60\,mg\,m^{-3}$ and higher), the use of reflectance ratios at wavelengths (670 nm, 704 nm) higher than the blue and green bands used in OC5 is more appropriate (Gons et al., 2002; Smith et al., 2018; Van der Zande et al., 2019). In very specific conditions, as those of microphytobenthos environment, OC5 may underestimate the Chl-*a* concentration. By construction, the Chl-*a* retrieved by OC5 tends to zero as SPM increases to very high levels. This is consistent with biogeochemical models in temperate coastal sea (Ford et al., 2017; Ménesguen et al., 2018) but could fail when applied to microphytobenthos growing on illuminated sediment and re-suspended in the water by the rising tide.

4.5.1. Implementation of OC5 in the processing CMEMS chain

The production of Chl-a images at Ifremer since 1998 has been entirely based on the application of the OC5 algorithm to coastal waters. The implementation of OC5 in the processing chain of the CMEMS project has provided a complete validation, a larger audience and a longer sustainability of the method (Saulquin et al., 2018). Daily interpolated products applying the OC5 algorithm to turbid waters have been operationally provided by ACRI-ST Company since 2015 within CMEMS. Over Europe the CMEMS/GlobColour product is 1 km of

spatial resolution and a similar product is also available at 4 km at global level. The full time series has been updated in November 2018 taking into account the availability of the new OLCI (Ocean and Land Colour Imager) sensor aboard Sentinel-3A (ESA), the R2018 processing of NASA, the CI and the OC5 algorithms for clear and coastal waters respectively (Garnesson et al., 2019). For the North Atlantic and Arctic oceans, the CMEMS/OC-CCI (ESA Climate Change Initiative) products are provided by PML (Plymouth Marine Laboratory) applying the regional OC5CI chlorophyll algorithm to multi-sensor reflectance. These multi-spectral reflectances are generated by merging the data from the SeaWiFS, MODIS-Aqua, MERIS, and VIIRS sensors and realigning the spectra to that of SeaWiFS. OC5CI is a combination of CI (open waters) and OC5 (coastal waters).

5. Conclusion

We used twenty years of satellite reflectance data from ESA and NASA ocean colour sensors in combination with *in situ* data to monitor changes in Chl-*a* in the English Channel and the northern Bay of Biscay on a 6-year basis, as requested by the European directives. The satellite data enhanced the spatial observations made at seven coastal stations. The Chl-*a* concentration showed a steady decline in the English Channel after the spring peak in April in the North and in May in the Bay of Seine whilst no trend or significant change was observed in the Bay of Biscay. Our results are in agreement with previous studies based on *in situ* data alone (Romero et al., 2013; Ratmaya et al., 2019), but extend the spatial frequency of observations required by Regional Sea Conventions or EU Directives (MSFD). However, some further questions on the decrease in Chl-*a* need to be answered; Is it only the result of lower discharges after the peaks observed in the early 2000s or an effect of altered ratios between nutrients (N/P and S/P) and a stronger limitation by phosphorus? To answer this question, the next few years will be particularly useful as the phosphorus content in the rivers will remain low and the release from sediment should decrease from year to year. For investigating the effect of river discharge on the phytoplankton biomass, a statistical model, based on the twenty two years of satellite Chl-*a* available to date, could be developed to relate the monthly outflows of major rivers to the Chl-*a* concentration on a pixel by pixel resolution, similarly to what has been done for the turbidity over the continental shelf of western Europe (Rivier et al., 2012; Gohin et al., 2015). This would also enable the assessment of the outputs of biogeochemical models and their calibration over years (Ménesguen et al., 2018). Using *in situ* and space-derived data together with modelling tools would provide a more comprehensive overview of the evolution of the coastal system as a whole, not only at the location of the seven stations selected in this study. This would also give us a better understanding of the role of climate on phytoplankton development; this study shows that adjacent seas can exhibit different responses to a similar climate, expressed from NAO and AMO indices. Further investigations of the composition of the phytoplankton, in term of size structure, Harmful Algal Blooms, diatoms to dinoflagellate ratios are also required. New phytoplankton indices, related to biological traits and life forms, are also very promising for monitoring the consequences of the decrease in phosphorus that could impact species with large cells, as proposed in Greenwood et al. (2019). A closer association between satellite and *in situ* data is therefore requested, not only to assess the performance of the satellite datasets, as we did in this study, but also to provide a better description of a changing coastal environment.

Acknowledgments

The authors thank the space agencies for having provided marine spectral reflectances: the NASA Goddard Space Flight Center, Ocean Ecology Laboratory, Ocean Biology Processing Group for SeaWiFS, MODIS/AQUA, VIIRS data and ESA for MERIS data. They are also grateful to eaufrance for providing river flows and nutrient concentration in the surface continental waters. The RHLN network is funded by the Seine-Normandy Water Agency and the Normandy Regional Council. This work has been carried out through the projects JMP-EUNOSAT (Joint Monitoring Programme of the Eutrophication of the North-Sea with Satellite data) funded by the DG ENV of the European Union (MSFD second cycle) and S3-EUROHAB (Sentinel-3 products for detecting EUtROphication and Harmful Algal Bloom events) funded by the European Regional Development Fund through the INTERREG France-Channel-England. This work has also been supported by the Ministère de la Transition écologique et Solidaire in France ("appui à la DCSMM").

References

Aminot, A., Kérouel, R., 2004. Hydrologie des écosystèmes marins. Paramètres et analyses. In Ifremer (ed), France.

Borja, A., Elliott, M., Carstensen, J., Heiskanen, A.S., van de Bund, W., 2010. Marine management – towards an integrated implementation of the European marine strategy framework and the water framework directives. Mar. Pollut. Bull. 60 (12), 2175–2186. https://doi.org/10.1016/j.marpolbul.2010.09.026.

Bryère, P., Mangin, A., Garnesson, P., 2019. Chlorophyll-a evolution during the last 20 years and its relation with mussel growth and optimal repartition for aquaculture and fishery. CMEMS Ocean State Report 3 (OSR3). Journal of Operational Oceanography. https://doi.org/10.1080/1755876X.2019.1633075. (in press).

Brylinski, J.M., Lagadeuc, Y., 1990. L'interface eaux côtières/eaux du large dans le Pas-de-Calais (côte française): une zone frontale. C. R. Seances Acad. Sci, 311 (II) 535–540.

Brylinski, J.M., Lagadeuc, Y., Gentilhomme, V., Dupont, J.P., Lafite, R., Dupeuple, P.A., Huault, M.F., Auger, Y., Puskaric, E., Wartel, M., Cabioch, L., 1991. Le fleuve côtier: un phénomène hydrologique important en Manche Orientale. Exemple du Pas-de-Calais. Oceanol. Acta 11, 197–203.

Campbell, J.W., 1995. The lognormal distribution as a model for bio-optical variability in the sea. J. Geophys. Res. 100 (C7), 13237–13254. https://doi.org/10.1029/95JC00458.

Capuzzo, E., Lynam CP, Barry J. et al. 2018. A decline in primary production in the North Sea over 25 years, associated with reductions in zooplankton abundance and fish stock recruitment. Glob Change Biol. 2018;24:e352–e364. doi:https://doi.org/10.1111/gcb.13916.

Chapelle, A., Lazure, P., Ménesguen, A., 1994. Modelling eutrophication events in a coastal ecosystem. Sensitivity analysis. Estuar. Coast. Shelf Sci. 39, 529–548. https://doi.org/10.1016/S0272-7714(06)80008-9.

Ferreira, J.G., Andersen, J.H., Borja, A., Bricker, S.B., Camp, J., Da Silva, M.C., Garces, E., Heiskanen, A.S., Humborg, C., Ignatiades, L., Lancelot, C., Ménesguen, A., Tett, P., Hoepffner, N., Claussen, U., 2011. Overview of eutrophication indicators to assess environmental status within the European marine strategy framework directive. Estuar. Coast. Shelf Sci. 93 (2), 117. https://doi.org/10.1016/j.ecss.2011.03.014.

Ford, D. A., van der Molen, J., Hyder, K., Bacon, J., Barciela, R., Creach, V. et al., 2017. Observing and modelling phytoplankton community structure in the North Sea. Biogeosciences, 14, 1419–1444. https//doi.org/10.5194/bg-14-1419-2017

Garnesson, P., Mangin, A., Fanton d'Andon, O., Demaria, J., Bretagnon, M., 2019. The CMEMS GlobColour chlorophyll-a product based on satellite observation: multi-sensor merging and flagging strategies. Ocean Sci. 15, 819–830. https://doi.org/10.5194/os-15-819-2019.

Goberville, E., Beaugrand, G., Sautour, B., Tréguer, P., SOMLIT Team, 2010. Climate-driven changes in coastal marine systems of western Europe. Mar. Ecol. Prog. Ser. 408, 129–148. https://doi.org/10.3354/meps08564.

Gohin, F., 2011. Annual cycles of chlorophyll-a, non-algal suspended particulate matter, and turbidity observed from space and in situ in coastal waters. Ocean Sci. 7, 705–732. https://doi.org/10.5194/os-7-705-201.

Gohin, F., Druon, J.N., Lampert, L., 2002. A five channel chlorophyll concentration algorithm applied to SeaWiFS data processed by Seadas in coastal waters. Int. J. Remote Sens. 23, 1639–1661. https://doi.org/10.1080/01431160110071879.

Gohin, F., Loyer, S., Lunven, M., Labry, C., Froidefond, J.M., Delmas, D., Huret, M., Herbland, A., 2005. Satellite-derived parameters for biological modelling in coastal waters: Illustration over the eastern continental shelf of the bay of biscay. Remote Sens. Environ. 95, 29–46. https://doi.org/10.1016/j.rse.2004.11.007.

Gohin, F., Saulquin, B., Oger-Jeanneret, H., Lozac'h, L., Lampert, L., Lefebvre, A., Riou, P., Bruchon, F., 2008. Towards a better assessment of the ecological status of coastal waters using satellite-derived chlorophyll-a concentrations. Remote Sens. Environ. 112, 3329–3340. https://doi.org/10.1016/j.rse.2008.02.014.

Gohin, F., Bryère, P., Griffiths, J.W., 2015. The exceptional surface turbidity of the north-west European shelf seas during the stormy 2013-2014 winter: Consequences for the initiation of the phytoplankton blooms? Journal of marine systems, 2015.148, 70-85, J. mar. In: Syst, https://doi.org/10.1016/j.jmarsys.2015.02.001.

Gómez-Jakobsen, F., Mercado, J.M., Cortés, D., Ramírez, T., Salles, S.Z., Yebra, L., 2016. A new regional algorithm for estimating chlorophyll-*a* in the Alboran Sea (Mediterranean Sea) from MODIS-aqua satellite imagery. Int. J. Remote Sens. 37 (6), 1431–1444. https://doi.org/10.1080/01431161.2016.1154223.

Gons, H.J., Rijkeboer, M., Ruddick, K.G., 2002. A chlorophyll-retrieval algorithm for satellite imagery (medium resolution imaging spectrometer) of inland and coastal waters. J. Plankton Res. 24 (9), 947–951. https://doi.org/10.1093/plankt/24.9.947.

Greenwood, N., Devlin, M.J., Best, M., Fronkova, L., Graves, CA., Milligan, A, Barry, J.,

van Leeuwen, SM., 2019, Utilizing Eutrophication Assessment Directives From Transitional to Marine Systems in the Thames Estuary and Liverpool Bay, UK., Front. Mar. Sci. 6:116. doi:0.3389/fmars.2019.00116.
Groetsch, P.M.M., Simis, S.G.H., Eleveld, M.A., Peters, S.W.M., 2016. Spring blooms in the Baltic Sea have weakened but lengthened from 2000 to 2014. Biogeosciences 13, 4959–4973. https://doi.org/10.5194/bg-13-4959-2016.
Harvey, E.T., Kratzer, S., Philipson, P., 2015. Satellite-based water quality monitoring for improved spatial and temporal retrieval of chlorophyll-a in coastal waters. Remote Sens. Environ. 158, 417–430. https://doi.org/10.1016/j.rse.2014.11.017.
Hernández Fariñas, T., Soudant, D., Barillé, L., Belin, C., Lefebvre, A., Bacher, C., 2014. Temporal changes in the phytoplankton community along the French coast of the eastern English Channel and the southern bight of the North Sea. ICES J. Mar. Sci. 71 (4), 821–833. https://doi.org/10.1093/icesjms/fst192.
Hu, C., Lee, Z., Franz, B., 2012. Chlorophyll a algorithms for oligotrophic oceans: a novel approach based on three-band reflectance difference. J. Geophys. Res. 117 (C1). https://doi.org/10.1029/2011jc007395.
Ifremer: Chlorophylle-a interpolée (données satellite) http://doi.org/10.12770/9352f74a-7ecb-485e-8ea3-9aa91001b9a1.
Jafar-Sidik, M., Gohin, F., Bowers, D., Howarth, J., Hull, T., 2017. The relationship between Suspended Particulate Matter and Turbidity at a mooring station in a coastal environment: consequences for satellite-derived products. Oceanologia 59 (3), 365–378. https://doi.org/10.1016/j.oceano.2017.04.003.
Karasiewicz, S., Breton, E., Lefebvre, A., Hernández Fariñas, T., Lefebvre, S., 2018. Realized niche analysis of phytoplankton communities involving HAB: Phaeocystis spp. as a case study. Harmful Algae 72, 1–13. https://doi.org/10.1016/j.hal.2017.12.005.
Kratzer, S., Harvey, T., Philipson, P., 2014. The use of ocean colour remote sensing in integrated coastal zone management-a case study from Himmerfjärden, Sweden. Mar. Policy 43, 29–39. https://doi.org/10.1016/j.marpol.2013.03.023.
Lacroix, G., Ruddick, K.G., Gypens, N., Lancelot, C., 2007. Modelling the relative impact of rivers (Scheldt/Rhine/Seine) and Western Channel waters on the nutrient and diatoms/*Phaeocystis* distributions in Belgian waters (Southern North Sea). Cont. Shelf Res. 27 (10–11), 1422–1446. https://doi.org/10.1016/j.csr.2007.01.013.
Lancelot, C., Passy, P., Gypens, N., 2014. Model assessment of present-day Phaeocystis colony blooms in the Southern North Sea (SNS) by comparison with a reconstructed pristine situation. Harmful Algae 37, 172–182. https://doi:10.1016/j.hal.2014.05.017.
Lapucci, C., Rella, M.A., Brandini, C., Ganzin, N., Gozzini, B., Maselli, F., Massi, L., Nuccio, C., Ortolani, A., Trees, C., 2012. Evaluation of empirical and semi-analytical chlorophyll algorithms in the Ligurian and North Tyrrhenian seas. J. Appl. Remote. Sens. 6 (1). https://doi.org/10.1117/1.JRS.6.063565.
Leadbetter, A., Silke, J., Cusack, C., 2018. Creating a weekly Harmful Algal Bloom bulletin. Marine Institute, Galway, Ireland.
Lefebvre, A., Guiselin, N., Barbet, F., Artigas, L.F., 2011. Long-term hydrological and phytoplankton monitoring (1992-2007) of three potentially eutrophicated systems in the eastern English Channel and the southern bight of the North Sea. ICES J. Mar. Sci. 68 (10), 2029–2043. https://doi.org/10.1093/icesjms/fsr149.
Loisel, H., Vantrepotte, V., Ouillon, S., Ngoc, D.D., Herrmann, M., Tran, V., Meriaux, X., Dessailly, D., Jamet, C., Duhaut, T., Nguyen, H.H., Nguyen, T.V., 2017. Variability over the Vietnamese coastal waters from the MERIS Ocean color sensor (2002 − 2012). Remote Sens. Environ. 190, 217–232. https://doi.org/10.1016/j.rse.2016.12.016.
Lorenzen, C.J., 1967. *Determination of chlorophyll and pheopigments* spectrophotometric equations. limnol. oceanogr. 12, 343–346.
Ménesguen, A., Desmit, X., Dulière, V., Lacroix, G., Thouvenin, B., Thieu, V., Dussauze, M., 2018. How to avoid eutrophication in coastal seas? A new approach to derive river-specific combined nitrate and phosphate maximum concentrations. Sci. Total Environ. 628–629, 400–414. https://doi.org/10.1016/j.scitotenv.2018.02.025.
Novoa, S., Chust, G., Sagarminaga, Y., Revilla, M., Borja, A., Franco, J., 2012. Water quality assessment using satellite-derived chlorophyll—a within the European directives, in the southeastern Bay of Biscay. Mar. Pollut. Bull. 65, 739–750. https://doi.org/10.1016/j.marpolbul.2012.01.020.
O'Reilly J. E, Werdell, P.J., 2019. Chlorophyll algorithms for ocean color sensors - OC4, OC5 & OC6, Remote Sensing of Environment,. Remote Sensing of Environment, 229, 32–47, doi:https://doi.org/10.1016/j.rse.2019.04.021.
O'Reilly, J.E., Maritorena, S., Mitchell, B.G., Siegel, D.A., Carder, K.L., Garver, S.A., Kahru, M., McClain, C.R., 1998. Ocean color chlorophyll algorithms for SeaWiFS. J. Geophys. Res. 103, 24937–24953. https://doi.org/10.1029/98JC02160.
OSPAR: Common procedure for the identification of the Eutrophication status of the OSPAR maritime area. Agreement 2013-08, 66p. https://www.ospar.org/work-areas/hasec/eutrophication/common-procedure
Passy, P., Gypens, N., Billen, G., Garnier, J., Thieu, V., Rousseau, V., Callens, J., Parent, J.Y., Lancelot, C., 2013. A model reconstruction of riverine nutrient fluxes and eutrophication in/the Belgian coastal zone since 1984. J. Mar. Syst. 128, 106–122. https://doi.org/10.1016/j.jmarsys.2013.05.005.
Ratmaya, W., Soudant, D., Salmon-Monviola, J., Cochennec-Laureau, N., Goubert, E., Andrieux-Loyer, F., Barillé, L., Souchu, P., 2019. Reduced phosphorus loads from the Loire and Vilaine rivers were accompanied by increasing eutrophication in the Vilaine Bay (South Brittany, France). Biogeosciences 16, 1361–1380. https://doi.org/10.5194/bg-16-1361-2019.
REPHY–French Observation and Monitoring program for Phytoplankton and Hydrology in coastal waters. REPHY Dataset - French Observation and Monitoring Program for Phytoplankton and Hydrology in Coastal Waters. vols. 1987-2016 Metropolitan data, 2017. SEANOE. http://doi.org/10.17882/47248
Rivier, A., Gohin, F., Bryère, P., Petus, C., Guillou, N., Chapalain, G., 2012. Observed vs. predicted variability in non-algal suspended particulate matter concentration in the English Channel in relation to tides and waves. Geo-Mar. Lett. 32 (2), 139–151. https://doi.org/10.1007/s00367-011-0271-x.
Romero, E., Garnier, J., Lassaletta, L., Billien, G., Le Gendre, R., Riou, P., 2013. Large-scale patterns of river inputs in southwestern Europe: seasonal and interannual variations and potential eutrophication effects at the coastal zone. Biogeochemistry 113, 481. https://doi.org/10.1007/s10533-012-9778-0.
Saulquin, B., Gohin, F., 2010. Mean seasonal cycle and evolution of the sea surface temperature from satellite and in situ data in the English Channel for the period 1986-2006. Int. J. Remote Sens. 31, 4069–4093. https://doi.org/10.1080/01431160903199155.
Saulquin, B., Gohin, F., Garrello, R., 2011. Regional objective analysis for merging high-resolution meris, modis/aqua, and seawifs chlorophyll-a data from 1998 to 2008 on the european Atlantic shelf. IEEE Trans. Geosci. Remote Sens. 49, 143–154. https://doi.org/10.1109/tgrs.2010.2052813.
Saulquin, F., Gohin, F., Fanton d'Andon, O., 2018. Interpolated fields of satellite-derived multi-algorithm chlorophyll-a estimates at global and European scales in the frame of the European Copernicus-marine environment monitoring service. Journal of Operational Oceanography. https://doi.org/10.1080/1755876X.2018.1552358.
Seegers, B.N., Stumpf, R.P., Schaeffer, B.A., Loftin, K.A., Werdell, P.J., 2018. Performance metrics for the assessment of satellite data products: an ocean color case study. Opt. Express 26 (6), 7404–7422. https://doi.org/10.1364/OE.26.007404.
Smith, M.E., Robertson Lain, L., Bernard, S., 2018. An optimized chlorophyll *a* switching algorithm for MERIS and OLCI in phytoplankton-dominated waters. Remote Sens. Environ. 215, 217–227. https://doi.org/10.1016/j.rse.2018.06.002.
SRN-Regional Observation and Monitoring program for Phytoplankton and Hydrology in the eastern English Channel. SRN dataset - Regional Observation and Monitoring Program for Phytoplankton and Hydrology in the eastern English Channel. 1992-2016, 2017. SEANOE. http://doi.org/10.17882/50832
Thomas, Y., Mazurié, J., Alunno-Bruscia, M., Bacher, C., Bouget, J.F., Gohin, F., Pouvreau, S., Struski, C., 2011. Modelling spatio-temporal variability of Mytilus edulis (L.) growth by forcing a dynamic energy budget model with satellite-derived environmental data. J. Sea Res. 66, 308–317. https://doi.org/10.1016/j.seares.2011.04.015.
Tilman, D., 1982. Resource Competition and Community Structure. Princeton University Press, New Jersey.
Tilstone, G., Mallor-Hoya, S., Gohin, F., Belo Couto, A., Sa, C., Goela, P., Cristina, S., Airs, R., Icely, J., Zühlke, M., Groom, S, 2017. Which ocean colour algorithm for MERIS in north west European waters? Remote Sens. Environ. 189, 132-151. https//doi.org/https://doi.org/10.1016/j.rse.2016.11.012
Van der Zande, D., Eleveld, M., Lavigne, H., Gohin, F., Pardo, S., Tilstone, G., Blauw, A., Markager, S., Enserink, L., (2019)(in press). Joint Monitoring Programme of the EUtrophication of the NOrth-Sea with SATellite data user case. CMEMS Ocean State Report 3 (OSR3). Journal of Operational Oceanography, in press, doi:https://doi.org/10.1080/1755876X.2019.1633075
Vanhoutte-Brunier, A., Fernand, L., Menesguen, A., Lyons, S., Gohin, F., Cugier, P., 2008. Modelling the karenia mikimotoi bloom that occurred in the western English channel during summer 2003. Ecol. Model. 210, 351–376. https://doi.org/10.1016/j.ecolmodel.2007.08.025.
Vermaat, J.E., McQuatters-Gollop, A., Eleveld, M.A., Gilbert, A., 2008. Past, present and future nutrient loads of the North Sea: causes and consequences. Est. Coast. Shelf Sci. 80 (1), 53–59. https://doi.org/10.1016/j.ecss.2008.07.005.
Wentzky, V.C., Tittel, J., Jäger, C.G., Rinke, K., 2018. Mechanisms preventing a decrease in phytoplankton biomass after phosphorus reductions in a German drinking water reservoir—results from more than 50 years of observation. Freshwater Biol. 63, 1063–1076. https://doi.org/10.1111/fwb.13116.